

The Graphs of Quantum Dilogarithm

Ivan C.H. Ip*

December 2, 2011

Abstract

Using the complex coloring method, we present the graphs of the quantum dilogarithm function $G_b(z)$ and visualize its analytic and asymptotic behaviors. In particular we demonstrate the limiting process when the modified $G_b(z) \rightarrow \Gamma(z)$ as $b \rightarrow 0$. We also survey the relations of $G_b(z)$ with different variants of the quantum dilogarithm function.

2010 Mathematics Subject Classification. Primary 33E, Secondary 20G42

Contents

1	Introduction	2
2	Complex Coloring	3
2.1	Specifications	3
2.2	Examples	4
3	The Quantum Dilogarithm $G_b(z)$	7
4	Visualizing $G_b(z)$ and $S_b(z)$	9
4.1	On the complex plane	9
4.2	Values along $z \in \mathbb{R}$	12
4.3	Values along imaginary direction	16
5	The Compact Quantum Dilogarithm	18
5.1	Visualizations	18
5.2	Limit of $\widehat{G}_b(z)$ to $\Gamma(z)$ as $b \rightarrow 0$	20
6	Relating $G_b(z)$ to other variants	23
	References	25

*Yale University, Department of Mathematics, 10 Hillhouse Avenue, New Haven, CT 06520, U.S.A.
Email: ivan.ip@yale.edu

1 Introduction

Let $q = e^{\pi i b^2}$ be the quantum parameter. The quantum dilogarithm function $G_b(z)$, defined for $b \in \mathbb{R}_{>0}$, is also known as the quantum exponential function or the hyperbolic gamma function. It bears its name from the properties of its variants $g_b(z)$ and $\Phi_b(z)$ given by

$$\Phi_b(z) = g_b(e^{2\pi b z}) = \frac{\overline{\zeta_b}}{G_b(\frac{Q}{2} - iz)}, \quad (1.1)$$

where $Q = b + b^{-1}$ and $\zeta_b = e^{\frac{\pi i}{2}(\frac{b^2+b^{-2}}{6} + \frac{1}{2})}$, such that

$$g_b(u)g_b(v) = g_b(u+v), \quad (1.2)$$

$$g_b(v)g_b(u) = g_b(u)g_b(q^{-1}uv)g_b(v) \quad (1.3)$$

hold for the positive self-adjoint Weyl type operators u, v with $uv = q^2vu$ in the case $|q| = 1$. The first relation says that it is a q -deformation of the exponential function, while the second relation is the deformed version of Roger's pentagon identity for the classical dilogarithm function. Using $\Phi_b(z)$, the pentagon relation can be written formally for the Heisenberg type operator $[p, x] = \frac{1}{2\pi i}$ as well by

$$\Phi_b(p)\Phi_b(x) = \Phi_b(x)\Phi_b(p+x)\Phi_b(p), \quad (1.4)$$

where we ignored the concerns of unboundedness and self-adjointness of operators.

On the other hand, the appearance of $G_b(z)$ in the q -binomial formula [3, 10] given by

$$(u+v)^{it} = b \int_{\mathbb{R}+i0} \frac{G_b(ib\tau - ibt)G_b(-ib\tau)}{G_b(-ibt)} u^{i\tau} v^{i(t-\tau)} d\tau, \quad (1.5)$$

where $uv = q^2vu$ as above, suggests that $G_b(bz)$ serves as the quantum analogue of the classical Gamma function. In fact it is shown in [10] that we have the limit given by

$$\lim_{r \rightarrow 0} \frac{G_b(bz)}{\sqrt{-i}|b|(1-q^2)^{x-1}} = \Gamma(z), \quad (1.6)$$

where we analytic continued b so that $b^2 = ir$ with $r > 0$ and the principal values of the complex powers are taken.

Faddeev's quantum dilogarithm function $\psi(z)$ is originally defined for $0 < q < 1$ using an infinite product expansion [5], and it is shown that it carries an analytic continuation to the regime $|q| = 1$, where the infinite product no longer converges, but instead an integral expression is found [6]. Since then a lot of variants have been defined in the literature serving different purposes. We have for example the

hyperbolic gamma function $\gamma(z)$ by Volkov [21], the quantum dilogarithm function $\Phi^\theta(z)$ by Fock-Goncharov [8], $V_\theta(z)$ by Woronowicz [22], and the 2-parameter G-function $G(a_+, a_-; z)$ given by Ruijsenaars [19]. This paper attempts to relate all these functions to the present choice of Teschner's definition of $G_b(z)$ in [3] so that the graphical presentations for this function can be translated to all these variants by shifting, stretching and phase changes easily.

The quantum dilogarithm function played a prominent role in the representation theory of noncompact quantum groups. This function and its many variants are being studied [9, 14, 19, 21] and applied to vast amount of different areas, for example the construction of the ' $ax + b$ ' quantum group by Woronowicz et.al. [18, 22], the harmonic analysis of the non-compact quantum group $U_q(\mathfrak{sl}(2, \mathbb{R}))$ and its modular double [3, 16, 17], the q -deformed Toda chains [15] and hyperbolic knot invariants [12]. Recently attempts have also been made to cluster algebra [8, 14] and quantization of the Teichmüller space [4, 7, 13]. One of the important properties of this function is its invariance under the duality $b \leftrightarrow b^{-1}$ that help encodes the detail of the modular double of the quantum plane [11], and also relates, for example, to the self-duality of Liouville theory [16].

The present paper is organized as follows. In Section 2, we introduce Jan Homann's representation of a complex valued function on the complex plane by a coloring method using a Mathematica code, and presents several examples illustrating this idea. Then in Section 3 we define $G_b(z)$ and describe its main analytic and asymptotic properties. In Section 4 we present the complex graphs $G_b(z)$ for several values of b , and its symmetric version $S_b(z)$. Then we restrict to the most interesting case along the real line and the imaginary direction and study its analytic and asymptotic properties. In Section 5, we present the graphs for the compact quantum dilogarithm corresponding to $\text{Re}(b^2) = 0$, and demonstrate using the complex graphs the limiting process of the modified $\widetilde{G}_b(z)$ tending towards the classical gamma function $\Gamma(z)$. Finally in Section 6, we relate $G_b(z)$ to all other variants of the quantum dilogarithm function used in the literature.

Acknowledgements. I would like to thank Alvin Wong and Hyun Kyu Kim for helpful discussions.

2 Complex Coloring

2.1 Specifications

We adopt the coloring method for a complex function developed by Jan Homann. The color function is obtained from the Mathematica code by Axel Boldt and can be found in [1].

In short, given a complex valued function defined on the complex plane, we represent the function by coloring the complex plane according to the following rules. The argument of a complex value is encoded by the hue of a color (red = positive real, and then counterclockwise through yellow, green, cyan, blue and purple; cyan stands for negative real). The absolute value of the function is represented by the brightness

and saturation of the color: strong colors denote points close to the origin, with black = 0, weak colors denote points with large absolute value, with white = ∞ .

The color is defined by 3 numbers ranging from 0 to 1. In the present coding, at the point $z = x + iy$ with value $f = f(x + iy)$, they are explicitly given by

$$Hue[h, s, b] := \left\{ \frac{Arg(f)}{2\pi}, \frac{1}{1 + 0.3 \ln(|f| + 1)}, 1 - \frac{1}{1.1 + 5 \ln(|f| + 1)} \right\}, \quad (2.1)$$

where h stands for hue, s the saturation and b the brightness.

The color function is hence given by Figure 1. We also note that taking inverse amounts to flipping the brightness of the color, and taking the opposite hue along the imaginary direction.

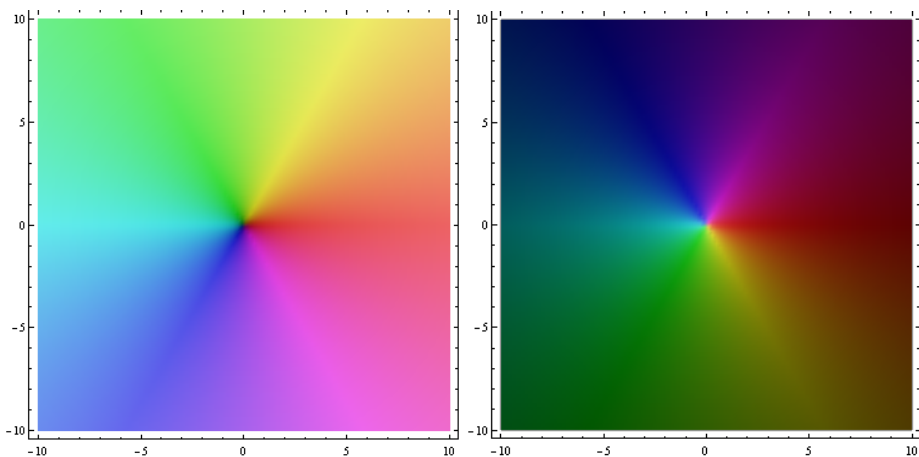


Figure 1: The color function for $f(z) = z$ and $f(z) = 1/z$

A good reference for the brightness of the color is given by the exponential function $f(z) = e^z$, see Figure 2.

2.2 Examples

Let us demonstrate the use of the complex coloring method. We illustrate here the graph of $f(z) = z^3$, the gamma function $f(z) = \Gamma(z)$ and the Riemann Zeta function $f(z) = \zeta(z)$.

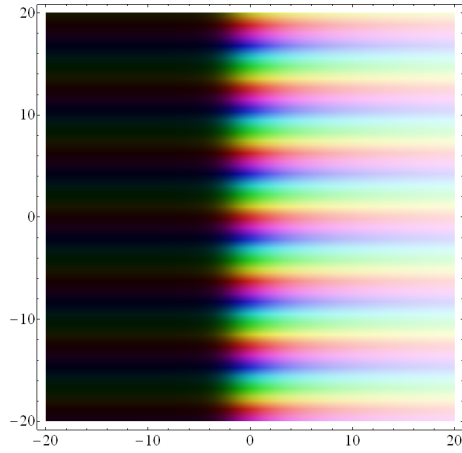


Figure 2: The brightness function for $f(z) = e^z$

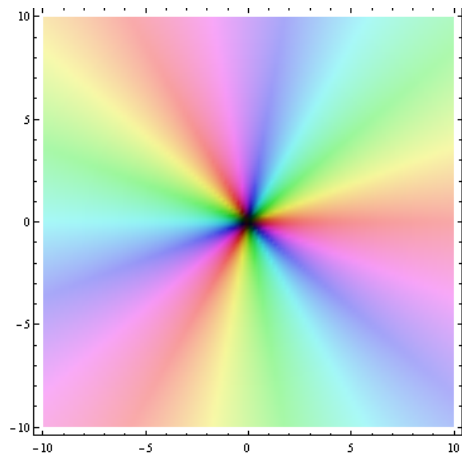


Figure 3: The graph of $f(z) = z^3$

From Figure 3, we observe that for $f(z) = z^3$ it has an order 3 zero, with the hue of color cycling around the point $z = 0$ for 3 times.

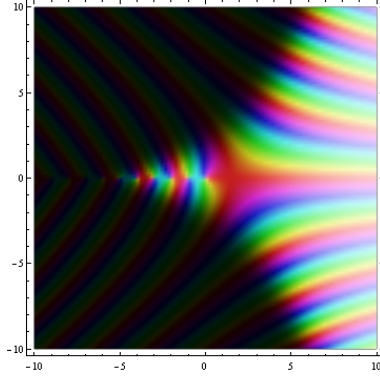


Figure 4: The graph of $f(z) = \Gamma(z)$

From Figure 4 for $f(z) = \Gamma(z)$, we observe the phase change behavior and the exponential growth along the imaginary direction. The few bright spot at $z = -n, n \in \mathbb{Z}_{\geq 0}$ indicates the simple poles.

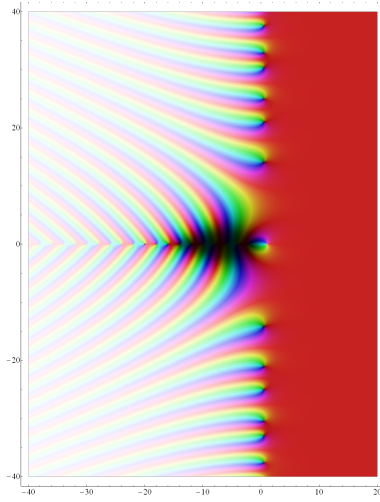


Figure 5: The graph of $f(z) = \zeta(z)$

From Figure 5 for $f(z) = \zeta(z)$, we observe the existence of nontrivial zeros along the line $Re(z) = \frac{1}{2}$, the trivial zeroes at $z = -2n, n \in \mathbb{Z}_{\geq 1}$ (where the color lines come together), the pole at $z = 1$, and the limit $\lim_{Re(z) \rightarrow +\infty} \zeta(z) = 1$.

3 The Quantum Dilogarithm $G_b(z)$

The quantum dilogarithm function can be defined in two ways. Historically it came from Barnes' double Zeta function [2] which is defined as follows:

Definition 3.1. Let $\omega := (w_1, w_2) \in \mathbb{C}^2$. The double Zeta function is defined as

$$\zeta_2(s, z|\omega) := \sum_{m_1, m_2 \in \mathbb{Z}_{\geq 0}} (z + m_1 w_1 + m_2 w_2)^{-s}. \quad (3.1)$$

The double Gamma function is defined as

$$\Gamma_2(z|\omega) := \exp \left(\frac{\partial}{\partial s} \zeta_2(s, z|\omega)|_{s=0} \right). \quad (3.2)$$

Let

$$\Gamma_b(x) := \Gamma_2(x|b, b^{-1}). \quad (3.3)$$

The quantum dilogarithm is defined as the function:

$$S_b(x) := \frac{\Gamma_b(x)}{\Gamma_b(Q - x)}, \quad (3.4)$$

where $Q = b + b^{-1}$.

The main object of study is the variant given by

$$G_b(x) := e^{\frac{\pi i}{2} x(Q-x)} S_b(x). \quad (3.5)$$

However for computational purpose, it is easier to use the equivalent integral form

Proposition 3.2. For $0 \leq \operatorname{Re}(z) \leq Q$, $G_b(z)$ can be expressed as

$$G_b(x) = \bar{\zeta}_b \exp \left(- \int_{\Omega} \frac{e^{\pi t z}}{(e^{\pi b t} - 1)(e^{\pi b^{-1} t} - 1)} \frac{dt}{t} \right), \quad (3.6)$$

where

$$\zeta_b = e^{\frac{\pi i}{2} (\frac{b^2 + b^{-2}}{6} + \frac{1}{2})}, \quad (3.7)$$

and the contour goes along \mathbb{R} with a small semicircle going above the pole at $t = 0$.

The integral converges absolutely for $0 < \operatorname{Re}(z) < Q$ and conditionally at the boundary.

The function G_b and S_b can be analytic continued to the whole complex plane as a meromorphic function, so that they have simple zeros at $z = Q + nb + mb^{-1}$ and simple poles at $z = -nb + -mb^{-1}$ for $n, m \in \mathbb{Z}_{\geq 0}$.

The quantum dilogarithm satisfies the following properties:

Proposition 3.3. *Self-duality:*

$$S_b(x) = S_{b^{-1}}(x), \quad G_b(x) = G_{b^{-1}}(x). \quad (3.8)$$

Functional equations:

$$S_b(x + b^{\pm 1}) = 2 \sin(\pi b^{\pm 1} x) S_b(x), \quad G_b(x + b^{\pm 1}) = (1 - e^{2\pi i b^{\pm 1} x}) G_b(x). \quad (3.9)$$

Reflection property:

$$S_b(x) S_b(Q - x) = 1, \quad G_b(x) G_b(Q - x) = e^{\pi i x(Q - x)}. \quad (3.10)$$

Complex conjugation:

$$\overline{S_b(x)} = \frac{1}{S_b(Q - \bar{x})}, \quad \overline{G_b(x)} = \frac{1}{G_b(Q - \bar{x})}, \quad (3.11)$$

in particular

$$\left| S_b\left(\frac{Q}{2} + ix\right) \right| = \left| G_b\left(\frac{Q}{2} + ix\right) \right| = 1 \text{ for } x \in \mathbb{R}. \quad (3.12)$$

Asymptotic properties:

$$G_b(x) \sim \begin{cases} \bar{\zeta}_b & \text{Im}(x) \longrightarrow +\infty, \\ \zeta_b e^{\pi i x(Q - x)} & \text{Im}(x) \longrightarrow -\infty, \end{cases} \quad (3.13)$$

where

$$\zeta_b = e^{\frac{\pi i}{4} + \frac{\pi i}{12}(b^2 + b^{-2})}. \quad (3.14)$$

Residues:

$$\lim_{x \rightarrow 0} x G_b(x) = \frac{1}{2\pi}, \quad (3.15)$$

or more generally,

$$\text{Res} \frac{1}{G_b(Q + z)} = -\frac{1}{2\pi} \prod_{k=1}^n (1 - q^{2k})^{-1} \prod_{l=1}^m (1 - \tilde{q}^{2l})^{-1} \quad (3.16)$$

at $z = nb + mb^{-1}$, $n, m \in \mathbb{Z}_{\geq 0}$ and $\tilde{q} = e^{\pi i b^{-2}}$.

Using the functional equation (3.9), the function can be extended to the whole complex plane using the integral formula (3.6) by

$$G_b(z + nQ) = G_b(x) \prod_{k=1}^n (1 - e^{2\pi i b(z + (k-1)Q)}), \quad (3.17)$$

$$G_b(z - nQ) = G_b(x) \prod_{k=1}^n (1 - e^{2\pi i b(z - kQ)})^{-1}, \quad (3.18)$$

where $n \in \mathbb{Z}_{\geq 0}$, $0 \leq \text{Re}(z) \leq Q$.

4 Visualizing $G_b(z)$ and $S_b(z)$

4.1 On the complex plane

Using the complex coloring method developed in Section 2, we obtained the graph for $G_b(x)$ for 2 random numbers $b = 0.7$ and $b = 0.248$ which suffice in showing the general shape of the function. We also considered the limiting case for $b = 1$. Due to slow convergence in the numerical calculation, we will consider another limiting case as $b = 0.1$ only in the next subsection when we restrict to the real line.

The graph of $G_b(z)$ for $b = 0.7$ is given in Figure 6, while the graph for $b = 0.248$ is given in Figure 7.

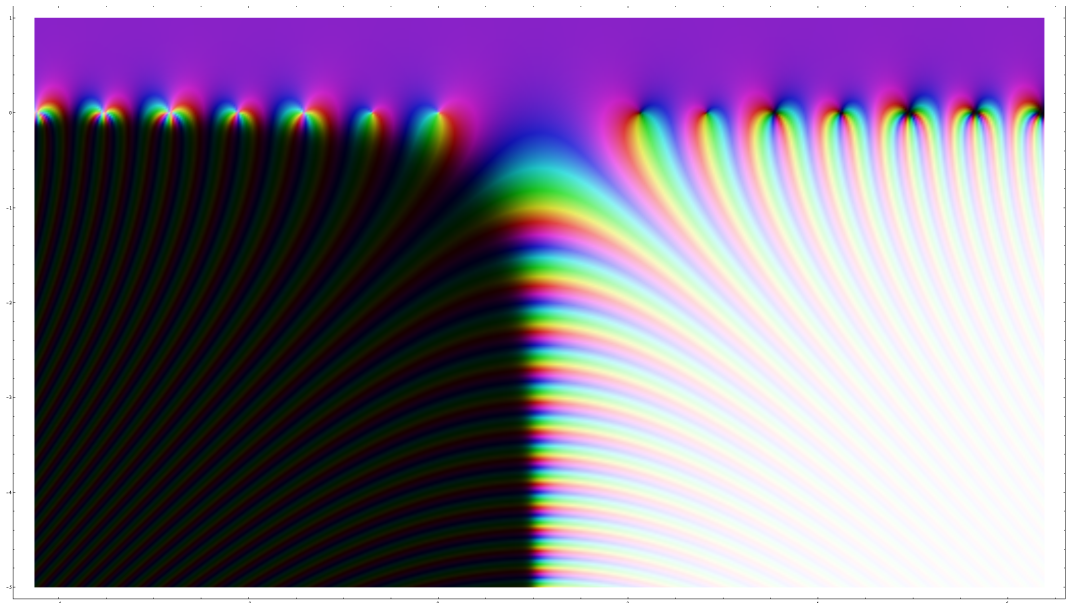


Figure 6: The graph of $G_b(z)$ for $b = 0.7, z \in [-2Q, 3Q] \times [-5, 1], Q = 2.129$

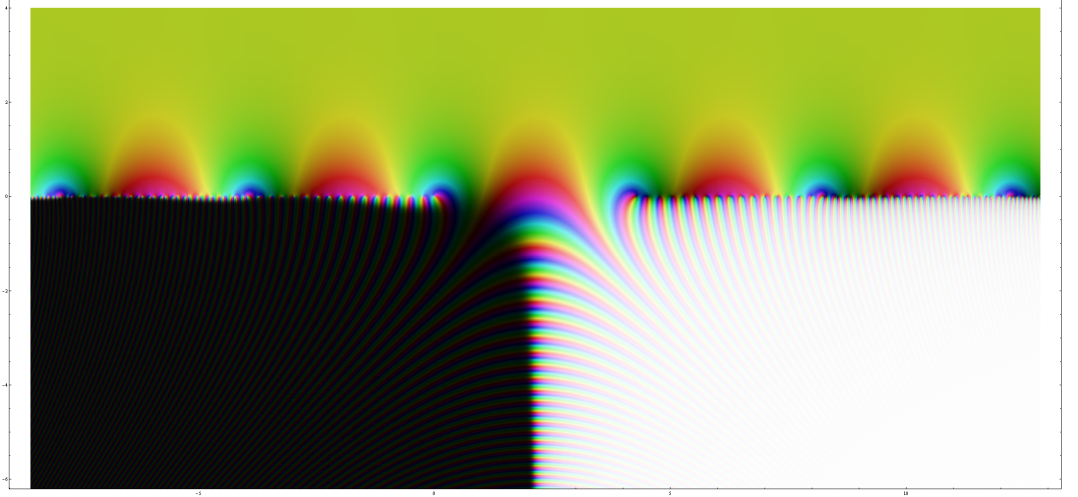


Figure 7: The graph of $G_b(z)$ for $b = 0.248, z \in [-2Q, 3Q] \times [-6, 4], Q = 4.280$

We immediately observe several properties

- We observe the symmetry along the axis $Re(z) = \frac{Q}{2}$, governed by the reflection properties (3.10). Furthermore, the poles and zeros along $Im(z) = 0$ are supposed to be simple, by comparing with the graph of $f(z) = z$ given in Section 2. The appearance of certain double or triple poles and zeros for the graph $b = 0.7$ comes from the fact that $b^{-1} \simeq 1.43 \sim 2b$, hence certain multiples $nb + mb^{-1}$ will come close together. For example, $z = 2b + 2b^{-1} = 4.257$ and $z = 4b + b^{-1} = 4.229$.
- It has exponential decay along the negative imaginary direction for $Re(z) < \frac{Q}{2}$, and exponential growth for $Re(z) > \frac{Q}{2}$. According to the asymptotic behavior from the last section, the growth is given by

$$|G_b(s + it)| = e^{-\pi t(2s - Q)}, \quad t \longrightarrow -\infty. \quad (4.1)$$

This also explains the brightness for different b when $Im(z) \longrightarrow -\infty$.

- On the other hand, it approaches the limit $\bar{\zeta}_b = e^{\pi i(b^2 + b^{-2} + 3)/12}$ in the positive imaginary direction.
- We observe the phase change along any given direction. In particular along $Re(z) = \frac{Q}{2}$ we do have the changes given according to $e^{\pi i z^2}$, increasing in frequency as $Im(z) \longrightarrow -\infty$.
- Finally let us note the similar shape compared with the Riemann Zeta function, which we believe is a coincidence.

It is also interesting to look at the limiting case for $b = 1$.

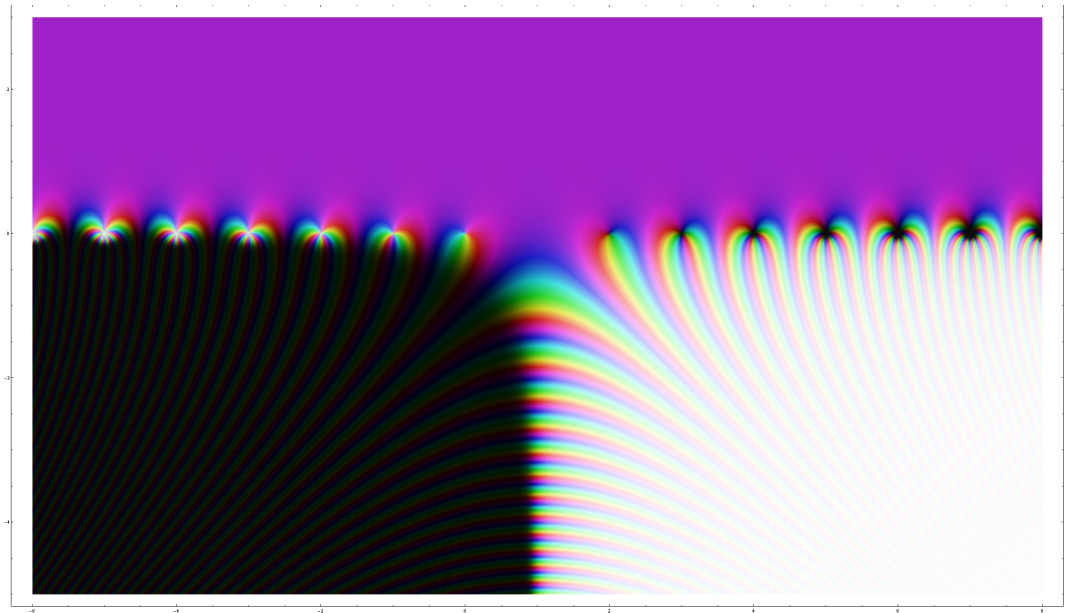


Figure 8: The graph of $G_b(z)$ for $b = 1, z \in [-2Q, 3Q] \times [-5, 3], Q = 2$

For the case $b = 1$, from Figure 8 we observe that the successive poles and zeroes have increasing order, due to the fact that b and b^{-1} coincide, which creates multiple poles. The poles at $z = -n$ and the zeroes at $z = 2 + n$ both have order $n + 1$ for $n = 0, 1, 2, \dots$

The graph can be made symmetric by considering $S_b(z)$ instead. The reflection properties give

$$S_b(z) = S_b(Q - z)^{-1}, \quad \overline{S_b(z)} = S_b(\bar{z}), \quad (4.2)$$

suggesting a full symmetry of the graph along $Re(z) = \frac{Q}{2}$ and $Im(z) = 0$. We illustrate the case for $b = 0.7$ in Figure 9.

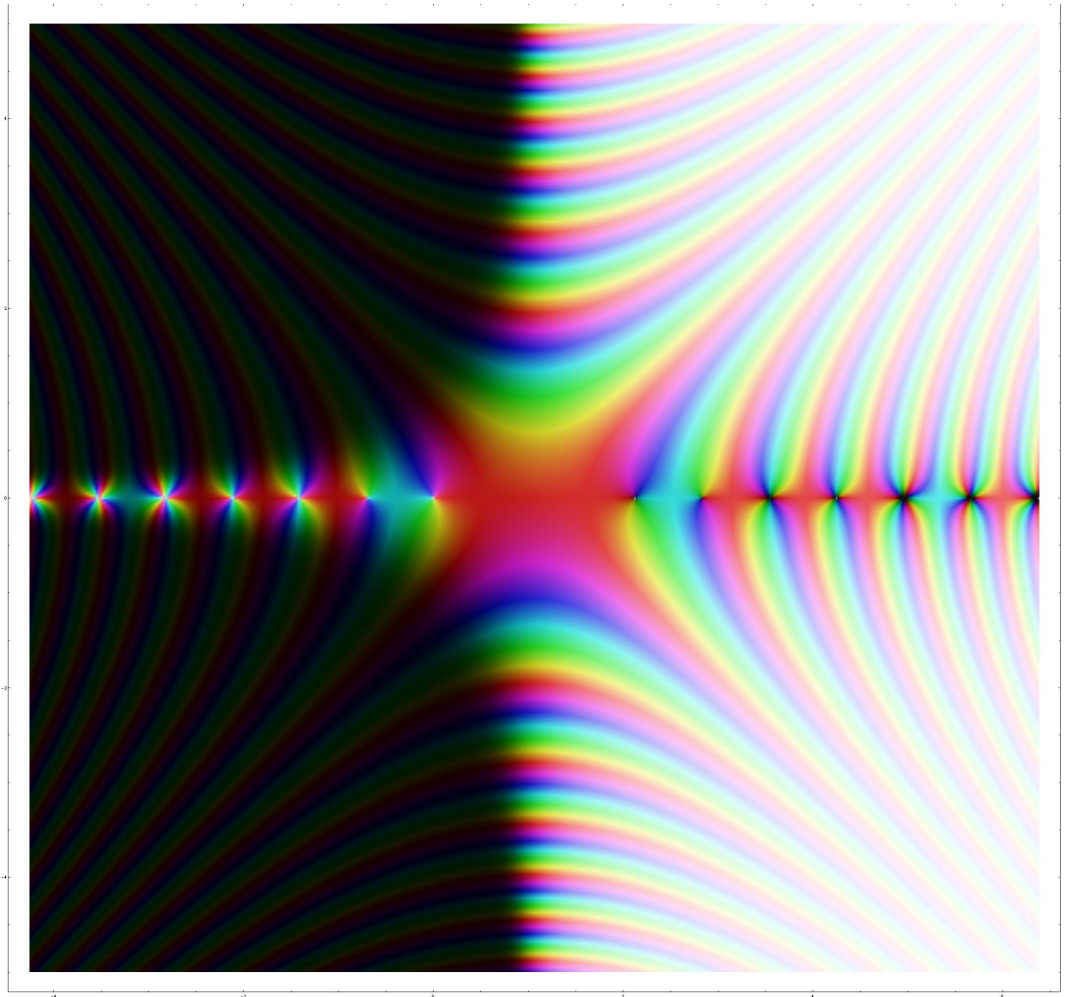


Figure 9: The graph of $S_b(z)$ for $b = 0.7$, $z \in [-2Q, 3Q] \times [-5, 5]$, $Q = 2.129$

4.2 Values along $z \in \mathbb{R}$

The most interesting behavior of the quantum dilogarithm appears at the real line, where all the poles and zeroes lie. Since we know that $\overline{S_b(z)} = S_b(\bar{z})$, we conclude that $S_b(z)$ takes real values when z is real. Therefore it suffices to plot the graphs for $S_b(z)$, and the values for $G_b(z)$ just amount to a phase change by the factor $e^{\pi iz(z-Q)/2}$ (cf. (3.5)).

Here we plot the graph for $b = 0.7$, $b = 0.248$ as well as the limiting case $b = 0.1$. Mathematica obtains a numerical overflow beyond this small value of b due to large exponential appearing in the integration of the definition, and the function is expected

to be quite badly behaved as the examples show.

The graph of $S_b(x)$ for $b = 0.7$ is given in Figure 10:

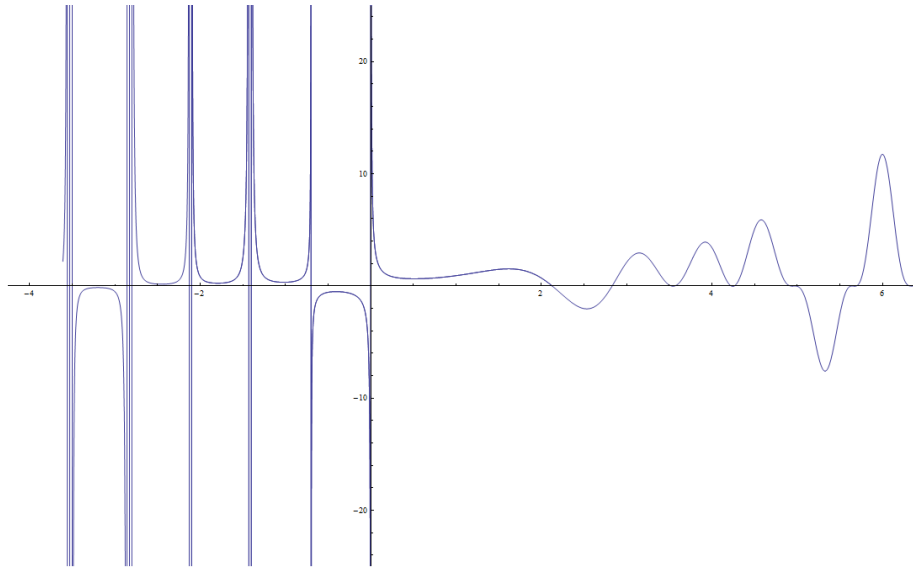


Figure 10: The graph of $S_b(x)$ for $b = 0.7$, $-2Q < x < 3Q$, $Q=2.129$

The graph of $S_b(x)$ for $b = 0.248$ is given in Figure 11:

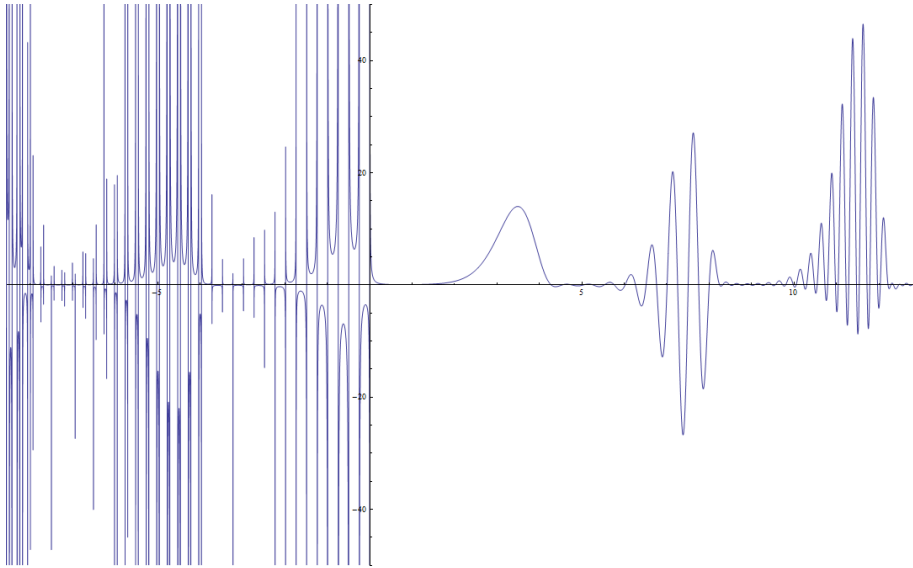


Figure 11: The graph of $S_b(x)$ for $b = 0.248$, $-2Q < x < 3Q$, $Q=4.280$

The graph of $S_b(x)$ for $b = 0.1$ is given in Figure 12:

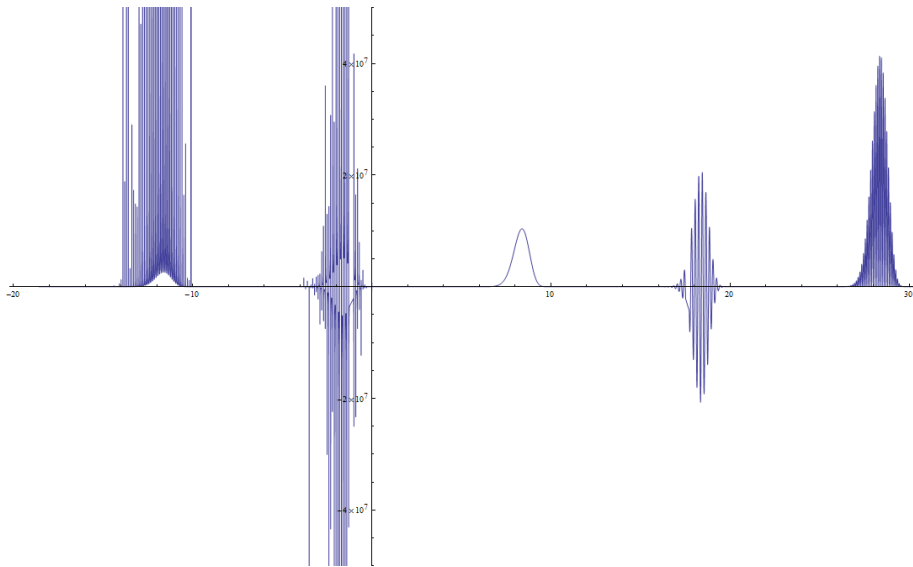


Figure 12: The graph of $S_b(x)$ for $b = 0.1$, $-2Q < x < 3Q$, $Q=10.1$

The case for $b = 0.1$ can be better illustrated by taking the log plot (of its absolute

values). From Figure 13, the spikes correspond to the position of the poles and zeroes.

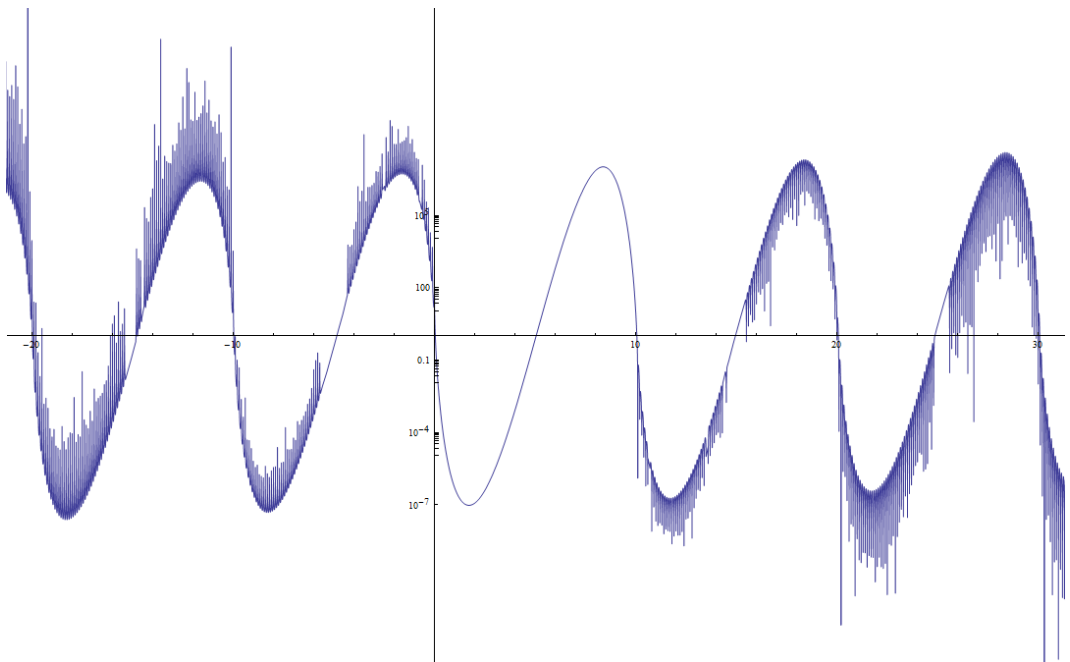


Figure 13: The logarithmic plot of $|S_b(x)|$ for $-2Q < x < 3Q$ and $b = 0.1$

Again let us comment on certain features of the graphs

- We can clearly observe the locations of the poles and zeroes. The zeroes are simple from the fact that the values of the function should alternate in signs. For $b = 0.7$, the appearance of a seemingly critical points comes from the fact that $b^{-1} = 1.429$ is quite close to $2b = 1.4$ as explained before.
- By the functional equation (3.9), the whole graph really depends on the portion $0 < x < Q$. The size of the bump governs the recurring amplitude of the graph by successive factor of 2, which comes from $2 \sin(\pi b) \sin(\pi b^{-1})$ appearing in the reflection properties for $S_b(x)$. This also explains the "periodicity" of the log plot for $b = 0.1$, which, in fact, has shifted by $\ln(2)$.
- The portion of the graph $0 < x < Q$ has exactly one local minimum and one local maximum for all values of b , and they are all positive real numbers. By taking the log plot in Figure 14, which essentially is the value of the integral, (we rescaled so that the endpoints at $x = 0$ and $x = Q$ matches), we see immediately that the size of the bump has a symmetric exponential relation along $x = \frac{Q}{2}$.

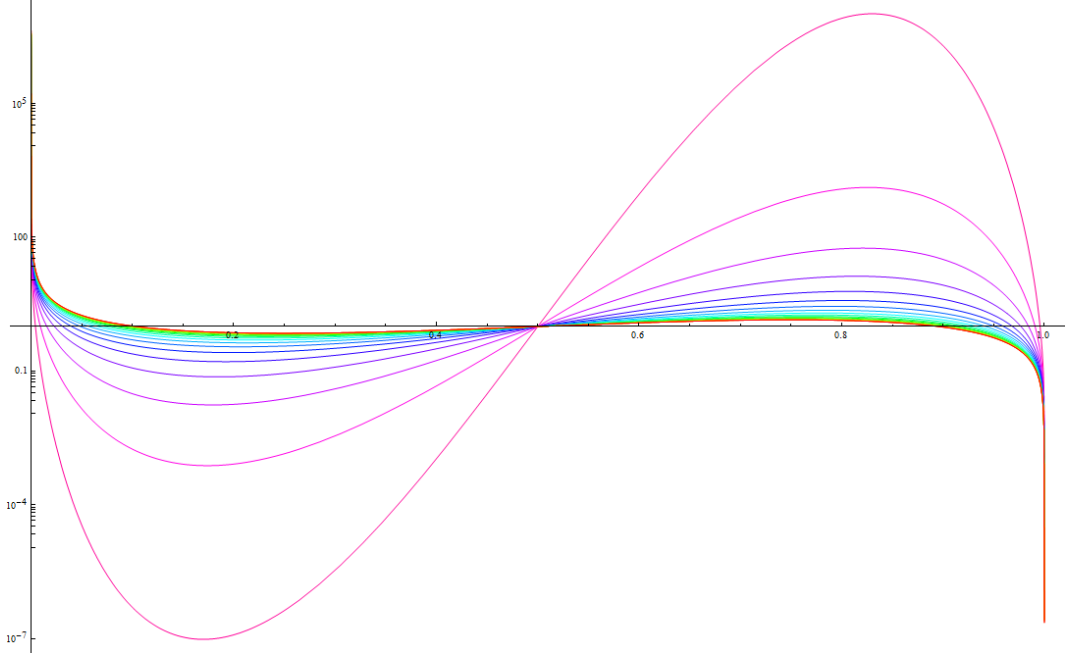


Figure 14: The logarithmic plot of $S_b(Qx)$ for $0 < x < 1$ and $b = 0.1$ to 1 in steps of 0.05

4.3 Values along imaginary direction

The values along the imaginary direction are simply governed by the asymptotic behavior. For completeness, we illustrate the graphs for $G_b(ix)$, $G_b(\frac{Q}{2} + ix)$ and $G_b(Q + ix)$ which appears quite often in the calculation of the representation theory of the quantum plane [11]. Again we choose $b = 0.7$. The absolute value is represented by a thick line, real value by a blue line, and imaginary value by a red line.

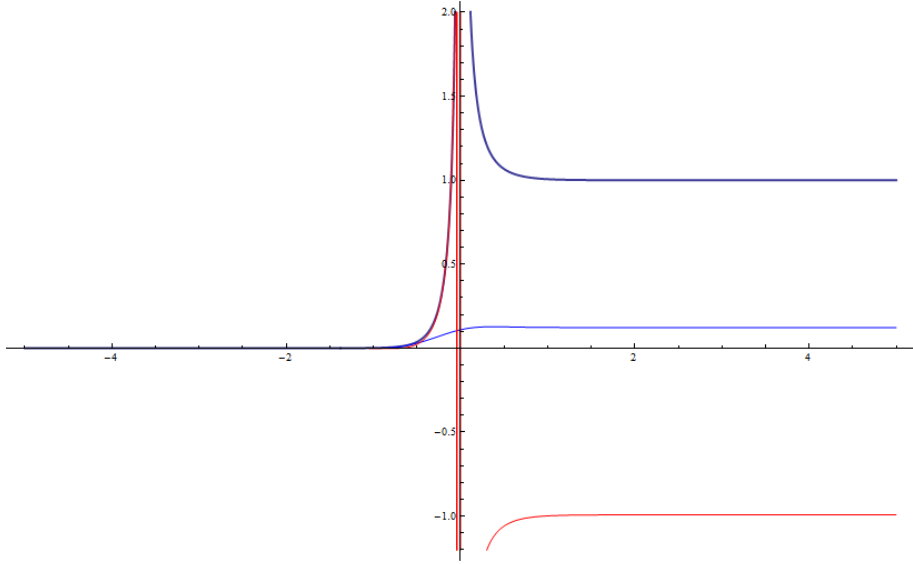


Figure 15: The graph of $G_b(ix)$ at $b = 0.7$ for $-5 < x < 5$

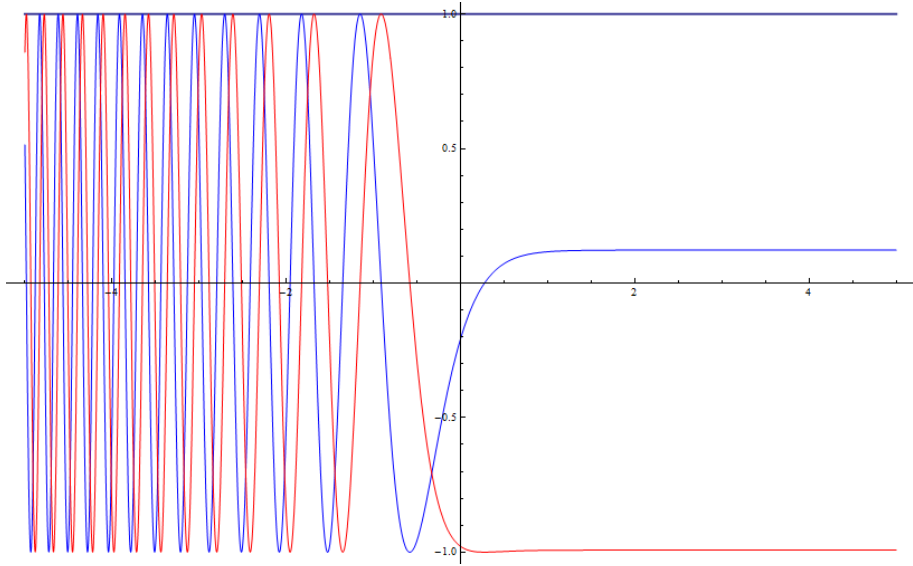


Figure 16: The graph of $G_b(\frac{Q}{2} + ix)$ at $b = 0.7$ for $-5 < x < 5$

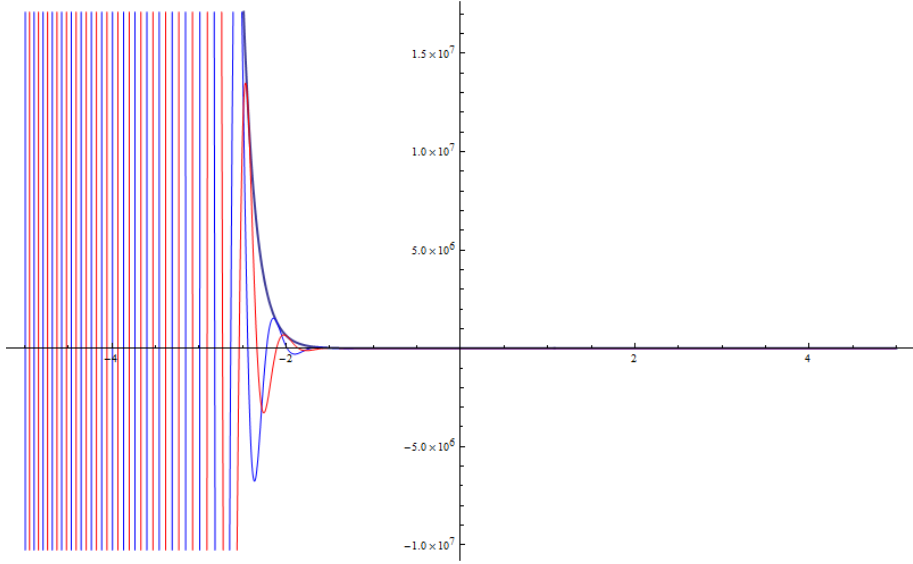


Figure 17: The graph of $G_b(Q + ix)$ at $b = 0.7$ for $-5 < x < 5$

- We observe the asymptotic behavior, that as $x \rightarrow \infty$, they all approach the complex number $\bar{\zeta}_b = 0.123 - 0.992i$.
- For $x \rightarrow -\infty$, $|G_b(ix)| \rightarrow e^{\pi Qx}$, while $|G_b(Q + ix)| \rightarrow e^{-\pi Qx}$. The relationship of the two graphs can easily be derived from the reflection properties (3.10).
- Finally $|G_b(\frac{Q}{2} + ix)| = 1$, and the asymptotic behavior for $x \rightarrow -\infty$ is $\bar{\zeta}_b e^{-\pi i \frac{Q^2}{4}} e^{-\pi ix^2}$, hence the increase in frequency is governed by πx^2 .

5 The Compact Quantum Dilogarithm

5.1 Visualizations

The analytic properties extend to the compact case, when $\text{Im}(b^2) > 0$, using an infinite product expansion, which we will call it the *compact quantum dilogarithm*:

Proposition 5.1. [20, Prop 5] For $\text{Im}(b^2) > 0$, we have the infinite product description

$$G_b(z) = \bar{\zeta}_b \frac{\prod_{n=1}^{\infty} (1 - e^{2\pi i b^{-1}(x - nb^{-1})})}{\prod_{n=0}^{\infty} (1 - e^{2\pi i b(x + nb)})}. \quad (5.1)$$

The location of the poles and zeroes are still the same, with poles at $-nb - mb^{-1}$, and zeroes at $Q + nb + mb^{-1}$ for $n, m = 0, 1, 2, \dots$

The most interesting case occurs when $b^2 = ir$ for $r > 0$, in which $0 < q = e^{\pi i b^2} < 1$. We establish the graph for $b = e^{\pi i/4} 0.7$ in Figure 18

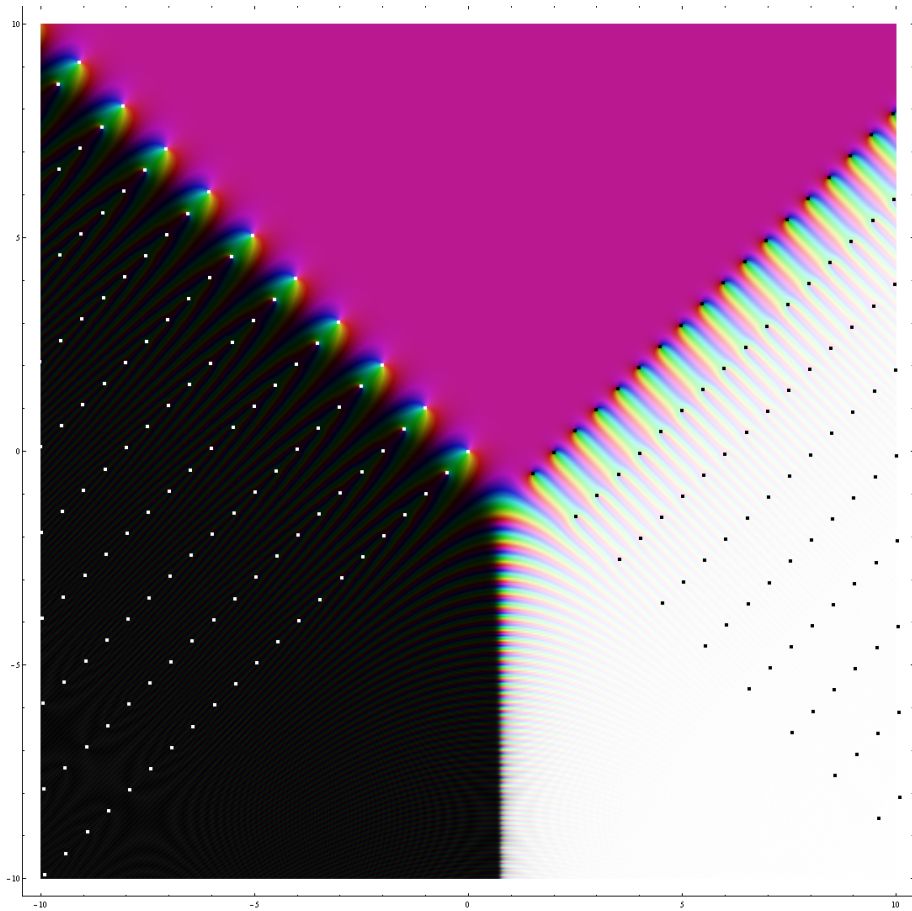


Figure 18: The graph of $G_b(z)$ at $b = e^{\pi i/4} 0.7$ for $z \in [-10, 10] \times [-10, 10]$

We have highlighted the zeroes with black dots and poles with white dots that align nicely together. We observe that the exponential decay and growth are extremely fast, due to the asymmetry bringing in a real part for the asymptotic $e^{\pi i z(z-Q)}$, thus giving a quadratic exponential growth.

The case for $b = e^{\pi i/4} 0.248$ illustrated in Figure 19 is less interesting due to the quick growth and decay of the function.

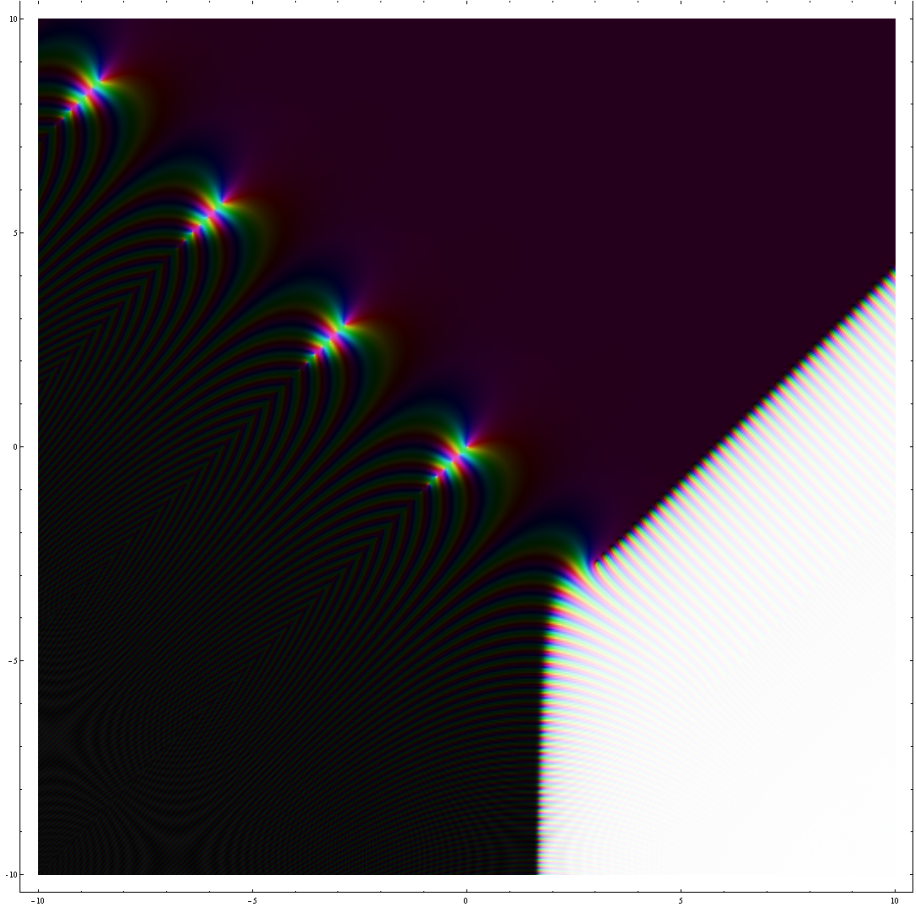


Figure 19: The graph of $G_b(z)$ at $b = e^{\pi i/4} 0.248$ for $z \in [-10, 10] \times [-10, 10]$

We observe that the separation of the poles is stretching out with increased exponential decay/growth compared with bigger $|b|$.

5.2 Limit of $\widetilde{G}_b(z)$ to $\Gamma(z)$ as $b \rightarrow 0$

Finally let us look at the theorem proved in [10]:

Theorem 5.2. *The following limit holds for $b^2 = ir \rightarrow i0^+$*

$$\lim_{r \rightarrow 0} \frac{G_b(bz)}{\sqrt{-i}|b|(1-q^2)^{x-1}} = \Gamma(z), \quad (5.2)$$

where $\sqrt{-i} = e^{-\frac{\pi i}{4}}$ and $-\frac{\pi}{2} < \arg(1-q^2) < \frac{\pi}{2}$.

Let us demonstrate the limiting process by considering the graph of the above function

$$\tilde{G}_b(z) := \frac{G_b(bz)}{\sqrt{-i|b|(1-q^2)^{z-1}}}. \quad (5.3)$$

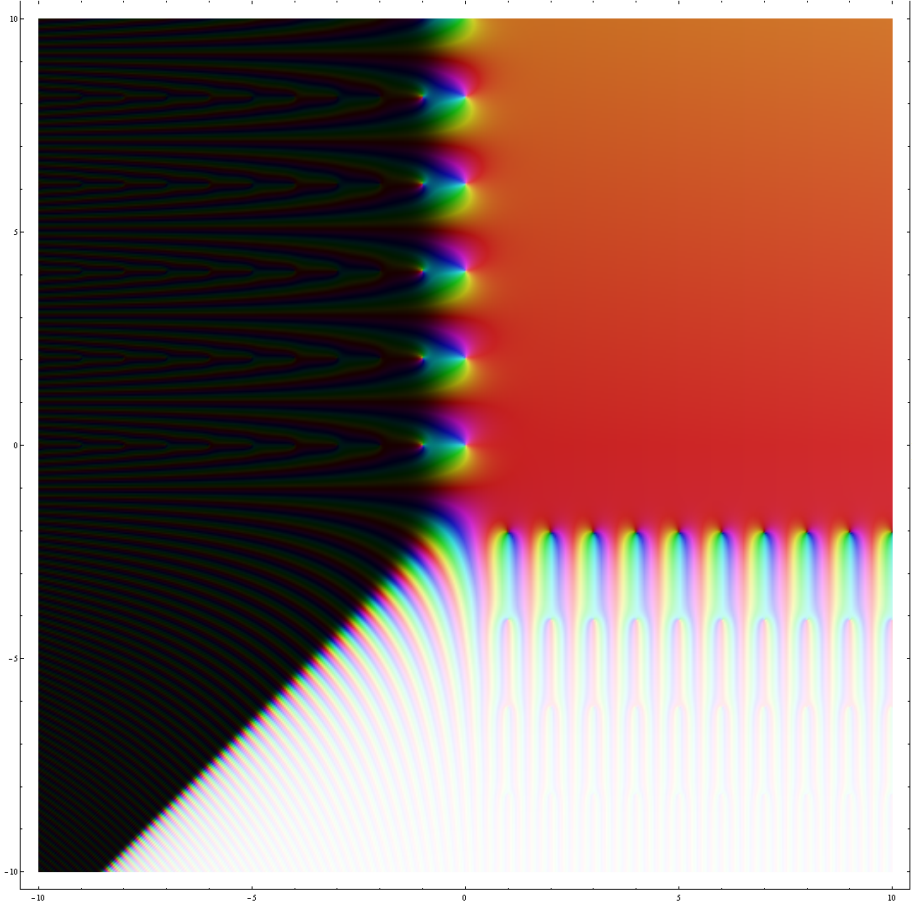


Figure 20: The graph of $\tilde{G}_b(z)$ at $b = e^{\pi i/4} 0.7$ for $z \in [-10, 10] \times [-10, 10]$

From Figure 20, we see that under multiplication by b in the argument, the zeroes and poles are aligned with the axis. The first zero occur at $z = \frac{Q}{b} = 1 - \frac{1}{|b|^2}i$. Now as $|b| \rightarrow 0$, we see that $\frac{Q}{b}$ moves downward and pushes away the zeroes and poles. It becomes clear in the graph for smaller $|b|$.

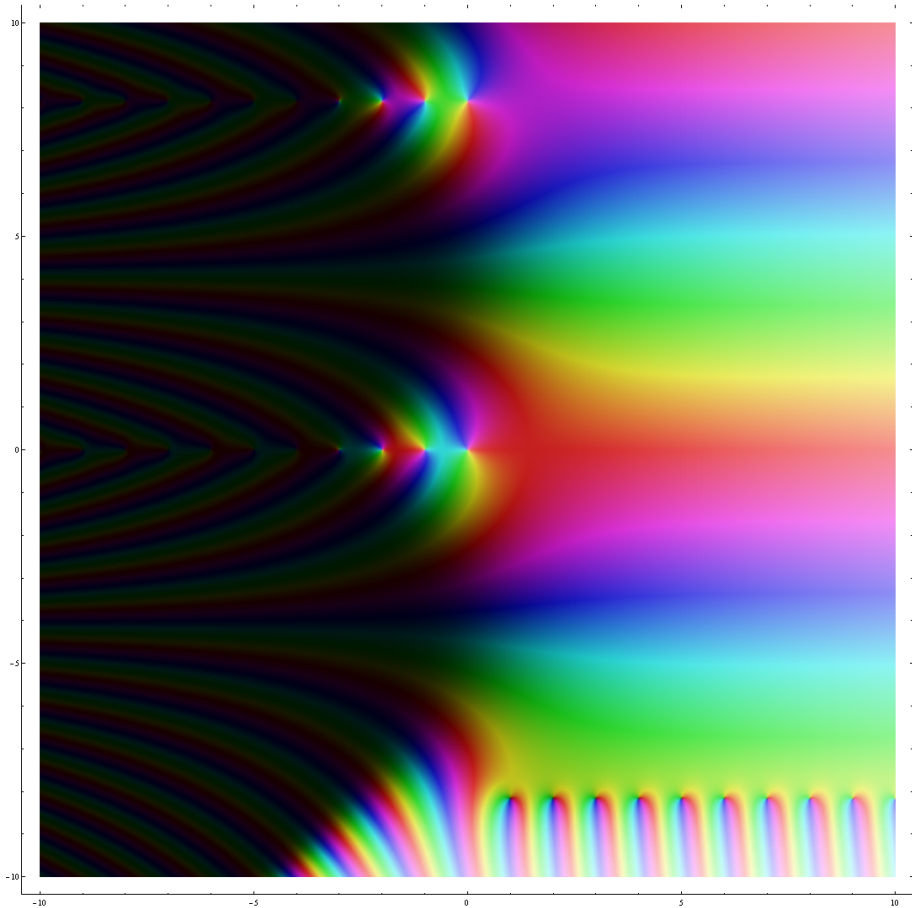


Figure 21: The graph of $\tilde{G}_b(z)$ at $b = e^{\pi i/4} 0.35$ for $z \in [-10, 10] \times [-10, 10]$

Now as $|b|$ becomes smaller, from Figure 21 we see that the small area around center begins to take shape with the poles and zeroes pushed away. Further reducing $|b|$ so that $\frac{Q}{b}$ is out of plotting range, we can see immediately in Figure 22 that indeed the graph resembles the Gamma function $\Gamma(z)$ given in Figure 4.

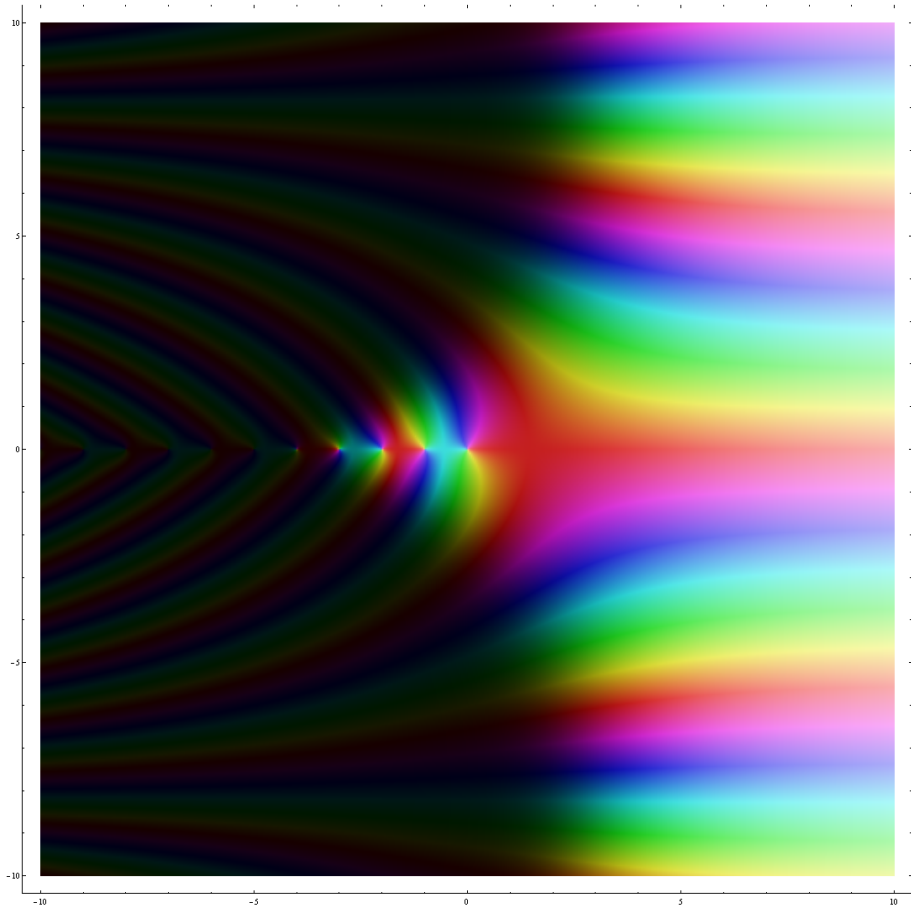


Figure 22: The graph of $\tilde{G}_b(z)$ at $b = e^{\pi i/4} 0.248$ for $z \in [-10, 10] \times [-10, 10]$

6 Relating $G_b(z)$ to other variants

We will see below that all variants of G_b amounts to shifting, scaling, taking inverses and multiplication by a constant. Hence the graphs of these variants can be obtained from those of $G_b(z)$ easily by shifting, stretching, and color phase changes.

The important function that satisfies the pentagon equation for Weyl-type operator is defined by

$$g_b(z) = \frac{\overline{\zeta_b}}{G_b(\frac{Q}{2} + \frac{\log z}{2\pi i b})}. \quad (6.1)$$

Lemma 6.1. *Let u, v be positive self-adjoint operators with $uv = q^2vu$, $q = e^{\pi i b^2}$.*

Then

$$g_b(u)g_b(v) = g_b(u+v), \quad (6.2)$$

$$g_b(v)g_b(u) = g_b(u)g_b(q^{-1}uv)g_b(v). \quad (6.3)$$

However, the graph of g_b which carries a branch cut at $x \in (-\infty, 0)$ is not particularly interesting, due to slow growth, and the fact that $-\pi < \text{Im}(\log z) < \pi$, so that

$$0 < \frac{Q}{2} - \frac{1}{2b} < \text{Re}\left(\frac{Q}{2} + \frac{\log z}{2\pi ib}\right) < \frac{Q}{2} + \frac{1}{2b} < Q, \quad (6.4)$$

and hence the argument in G_b never hits any zeroes or poles.

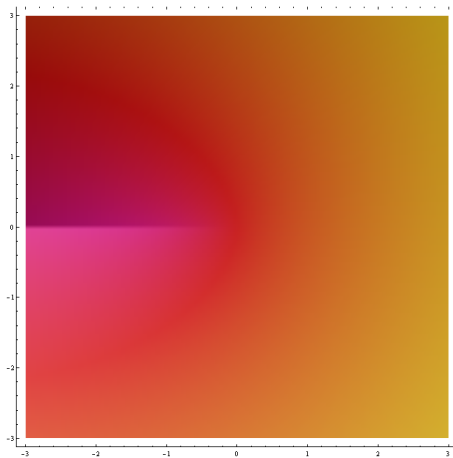


Figure 23: The graph of $g_b(z)$ for $b = 0.7$ for $z \in [-3, 3] \times [-3, 3]$

The quantum dilogarithm $G_b(x)$ defined above has real b as parameters. Although the integral formula can be analytically continued to complex b with positive real part, we recall that the function coincide with the *compact quantum dilogarithm* given in Prop 5.1:

$$G_b(z) = \zeta_b^- \frac{\prod_{n=1}^{\infty} (1 - e^{2\pi i b^{-1}(x - nb^{-1})})}{\prod_{n=0}^{\infty} (1 - e^{2\pi i b(x + nb)})}. \quad (6.5)$$

From this we can compare with $\gamma(z)$ defined by Volkov [21]:

Definition 6.2. Let $q = e^{\pi i \tau}$ for $\text{Im}(\tau) > 0$. Then the hyperbolic Gamma function is defined by

$$\gamma(z) := \frac{(q^2 e^{-2\pi i z}; q^2)_{\infty}}{(e^{-2\pi i z/\tau}; q^{-2/\tau^2})_{\infty}}. \quad (6.6)$$

Proposition 6.3. *With $\tau = b^2$, we have*

$$\gamma(z) = \overline{\zeta}_b G_b(Q - \frac{z}{b})^{-1}. \quad (6.7)$$

The infinite product expansion is also involved in the original definition ψ_b by Faddeev [6]:

Definition 6.4. *Let $s_q(w) = \prod_{n=0}^{\infty} (1 + q^{2n+1}w)$ and define*

$$\psi(p) := \frac{s_q(e^{bp})}{s_{\tilde{q}}(e^{p/b})}, \quad (6.8)$$

where $\tilde{q} = e^{\pi i b^{-2}}$. Then $\psi(p)$ admits the integral expansion

$$\psi(p) := \exp \left(\frac{1}{4} \int_{\Omega} \frac{e^{ip\xi/\pi}}{\sinh(b\xi) \sinh(\xi/b)} \frac{d\xi}{\xi} \right). \quad (6.9)$$

Fock-Goncharov [8] used a similar variant Φ^{\hbar} , which is the same as V_{θ} used by Woronowicz-Zakrzewski's [22]:

Definition 6.5.

$$\Phi^{\hbar}(z) := \exp \left(-\frac{1}{4} \int_{\Omega} \frac{e^{-ipz}}{\sinh(\pi p) \sinh(\pi \hbar p)} \frac{dp}{p} \right), \quad (6.10)$$

$$V_{\theta}(z) := \exp \left(\frac{1}{2\pi i} \int_0^{\infty} \log(1 + x^{-\theta}) \frac{dx}{x + e^{-z}} \right). \quad (6.11)$$

The we have the relations

Proposition 6.6.

$$V_{b^{-2}}(z) = \Phi^{b^2}(z) = g_b(e^z)^{-1} = \zeta_b G_b \left(\frac{Q}{2} - \frac{iz}{2\pi b} \right), \quad (6.12)$$

$$\psi(z) = \Phi^{b^2}(-bz)^{-1} = \gamma(b(Q + \frac{z}{2\pi i})) = \overline{\zeta}_b G_b \left(\frac{Q}{2} + \frac{iz}{2\pi} \right)^{-1}. \quad (6.13)$$

Finally, a more general version with two parameters is given by Ruijinaars [19]

Lemma 6.7. *Let a_-, a_+ be two positive real numbers. Ruijinaars's G function is defined by*

$$G(a_+, a_-; z) := \exp \left(i \int_0^{\infty} \frac{dy}{y} \left(\frac{\sin 2yz}{2 \sinh(a_+ y) \sinh(a_- y)} - \frac{z}{a_+ a_- y} \right) \right), \quad (6.14)$$

with $|Im(z)| < (a_+ + a_-)/2$ and extend meromorphically to the whole complex plane. Then

$$G(b, b^{-1}; z) = S_b \left(\frac{Q}{2} - iz \right). \quad (6.15)$$

References

- [1] A. Boldt, *Mathematica 6.0 code to graph complex functions*, <http://math-www.uni-paderborn.de/~axel/graphs/>
- [2] E.W. Barnes, *The theory of the double gamma function*, Philos. Trans. Roy. Soc., A196:265388, (1901)
- [3] A.G. Bytsko, K. Teschner, *R-Operator, co-product and Haar-measure for the modular double of $U_q(\mathfrak{sl}(2, \mathbb{R}))$* , Comm. Math. Phys. **240**, 171-196, (2003)
- [4] L. Chekhov, V.V. Fock, *A quantum Teichmüller space*, Theor. Math. Phys. **120**, 511-528, (1999)
- [5] L.D. Faddeev, *Discrete Heisenberg-Weyl group and modular group*, Lett. Math. Phys. **34**, 249-254, (1995)
- [6] L.D. Faddeev, R.M. Kashaev, *Quantum dilogarithm*, Modern Phys. Lett. **A9**, 427-434, (1994)
- [7] I. Frenkel, H. Kim, *Quantum Teichmüller space from quantum plane*, arXiv:1006.3895v1, (2010)
- [8] V.V.Fock, A.B. Goncharov, *The quantum dilogarithm and representations of quantized cluster varieties*, Inv. Math. **175** No. 2, 223-286, (2009)
- [9] A. B. Goncharov, *Pentagon relation for the quantum dilogarithm and quantized $\mathcal{M}_{0,5}^{cyc}$* , Progress in Mathematics, **256**, 413-426, (2007)
- [10] I. Ip, *The classical limit of representation theory of the quantum plane*, arXiv:1012.4145, (2010)
- [11] I. Ip, *Representation of the quantum plane, its quantum double and harmonic analysis on $GL_q^+(2, \mathbb{R})$* , arXiv:1108.5365, (2011)
- [12] R.M. Kashaev, *The hyperbolic volume of knots from the quantum dilogarithm*, Lett. Math. Phys. **39**, 269-275, (1997)
- [13] R.M. Kashaev, *Quantization of Teichmüller spaces and the quantum dilogarithm*, Lett. Math. Phys. **43**, 105-115, (1998)
- [14] R.M. Kashaev, T. Nakanishi, *Classical and quantum dilogarithm identities*, arXiv:1104.4630, (2011)
- [15] S. Kharchev, D. Lebedev, M. Semenov-Tian-Shanksy, *Unitary representations of $U_q(\mathfrak{sl}(2, \mathbb{R}))$, the modular double, and the multiparticle q -deformed Toda chain*, Comm. Math. Phys. **225**(3), 573-609, (2002)
- [16] B. Ponsot, J. Teschner, *Liouville bootstrap via harmonic analysis on a noncompact quantum group*, arXiv: hep-th/9911110, (1999)

- [17] B. Ponsot, J. Teschner, *Clebsch-Gordan and Racah-Wigner coefficients for a continuous series of representations of $\mathcal{U}_q(\mathfrak{sl}(2, \mathbb{R}))$* , Comm. Math. Phys. **224**, 613-655, (2001)
- [18] W. Pusz, S.L. Woronowicz, *A new quantum deformation of 'ax+b' group*, Comm. Math. Phys. **259**, 325-362, (2005)
- [19] S.N.M. Ruijsenaars, *A unitary joint eigenfunction transform for the $A\Delta O$'s $\exp(ia_{\pm}d/dz) + \exp(2\pi z/a_{\mp})$* , J. Nonlinear Math. Phys. **12** Suppl. 2, 253-294, (2005)
- [20] T. Shintani, *On a kronecker limit formula for real quadratic fields*, J. Fac. Sci. Univ. Tokyo Sect. 1A Math. **24**, 167-199, (1977)
- [21] A.Yu. Volkov, *Noncommutative hypergeometry*, Comm. Math. Phys. **258**(2), 257-273, (2005)
- [22] S.L.Woronowicz, S. Zakrzewski, *Quantum 'ax + b' group*, Reviews in Mathematical Physics, **14**, 7&8, 797 - 828, (2002)